





Research article

UDC 624.97

DOI: 10.34910/MCE.138.1



## Numerical analysis of Arctic wind turbines supporting structures

I.V. Rigel  , V.V. Elistratov 

*Peter the Great St. Petersburg Polytechnic University, St. Petersburg, Russian Federation*

 [ivan.rigel@yandex.ru](mailto:ivan.rigel@yandex.ru)

**Keywords:** Arctic wind turbine, environmental conditions, supporting structures, numerical modeling, stress-strain state, dynamic response, permafrost degradation, ground reaction forces

**Abstract.** The paper presents numerical modeling methods for the supporting structures of wind turbines operating under Arctic conditions on permafrost soils. The relevance of the research is determined by the strategic priorities for the development of the Russian Arctic zone and the need to consider the specific environmental and climatic conditions in the energy infrastructure design. An integrated methodology is developed for analyzing the structural behavior of Arctic wind turbines, including the stress–strain state and dynamic response of the supporting structures finite element modeling, accounting for wind and operational loads, nonlinear soil–structure interaction, thermal regime, and temperature-dependent soil properties. The methodology is tested through a case study of a 100 kW wind turbine with a 30 m tower and a 24 m rotor diameter, for the Yamal-Nenets Autonomous Okrug environmental conditions. The results show that the permafrost degradation leads to increased displacements and stresses in the structural system by up to 25 % and reduces the structure natural frequencies by up to 10 %, due to a local 70-fold decrease in reactive soil resistance. The identified factors should be considered in the Arctic wind turbines design to ensure accurate assessment of structural performance and resonance risks.

**Funding:** The research was supported by the Russian Science Foundation grant No. 25-29-00497, <https://rscf.ru/project/25-29-00497/>.

**Citation:** Rigel, I.V., Elistratov, V.V. Numerical analysis of Arctic wind turbines supporting structures. Magazine of Civil Engineering. 2025. 18(6). Article no. 13801. DOI: 10.34910/MCE.138.1

### 1. Introduction

Wind turbines are structures that convert wind energy into electricity and represent a promising solution for remote regions of the Arctic, where energy supply is predominantly provided by diesel power plants. This results in high energy costs due to the logistical challenges of fuel delivery and has a negative environmental impact. The potential of Arctic wind energy is supported by the presence of strong and stable winds in northern regions [1]. According to forecasts [2], wind energy potential in the Russian Arctic is expected to increase throughout the 21<sup>st</sup> century, while the frequency of wind speeds outside the operational range of wind turbines will decrease across much of Eastern Siberia, thereby improving the capacity factor. These trends create long-term prospects for the deployment of Arctic wind power systems; however, the extreme climatic conditions of the Russian Arctic present significant engineering challenges.

One of the key characteristics of the object under study is the installation of wind turbines on permafrost ground, i.e., soils that remain in a frozen state for three or more years and ensure the stability of the supporting structural system in its design position. The loads acting on the supporting structure of a wind turbine are balanced by reactive forces from the soil, which depend on its physical and mechanical properties. Studies have shown that climate warming, occurring faster in the Arctic than the global average [3], leads to permafrost thawing, posing a threat to the reliable operation of infrastructure, including wind turbines. Permafrost degradation manifests itself in the deepening of the seasonally thawed layer and the change of the physical and mechanical properties of permafrost soils due to temperature increase, which

can lead to excessive settlements, tilting, loss of stability of wind turbines and increased static and dynamic loads on structural elements [4, 5]. This phenomenon is recognized as one of the critical factors affecting the reliability and durability of building structures in permafrost zones, since the reduction of bearing capacity and stiffness of the ground compromises structural performance and may lead to emergency condition of structure [6]. The study of these aspects is essential for the development of adapted structural solutions that ensure the safe and stable operation of wind turbines under Arctic conditions.

Wind turbines are subjected to dynamic loads resulting from wind gusts and rotor rotation, which induce structural vibrations. Environmental factors such as icing, snow, seasonal and long-term changes in permafrost properties affect the natural frequencies of the wind turbine and its structural elements [5, 7, 8]. A reduction of the supporting structures fixation stiffness, increased mass and inertia of the rotor and nacelle assembly (RNA) due to icing and snow loads, leads to system natural frequencies decrease and an amplification of its dynamic response. If the structure natural frequencies approach the frequencies of external loads, resonance may occur, which can lead to an emergency condition of the wind turbine. As noted in [9], neglecting the ground–structure interaction leads to distorted estimations of internal forces in the superstructure and does not allow for an accurate assessment of displacements. Accounting the ground stiffness is particularly important when developing damping devices to mitigate wind and seismic loads acting on the structure [4, 10].

Modern research in wind turbine design focuses on aerodynamic blades modeling, wind-induced loads assessment, evaluation of the static stress–strain state (SSS) and analysis of the supporting structural systems dynamic response. To this end, numerical methods and specialized software are employed for aeroservoelastic modeling of wind turbines, including OpenFAST and QBlade, as well as finite element software packages for structural mechanics simulations, such as ANSYS Mechanical, Abaqus, SAP2000 and others [4, 11–22].

Nonlinear boundary conditions allow for a more realistic representation of soil response and enable more accurate prediction of the behavior of wind turbine support structures under loading, which is essential for developing reliable and durable designs in Arctic environments. The fixation stiffness in calculation schemes of wind turbines can be incorporated using various approaches. Most studies related to the modeling of fixation conditions refer to offshore wind turbines with monopile foundations [23–26]. In [24], the primary modern methods for modeling soil–structure interaction in wind turbine analysis are presented, including the apparent fixity method, coupled spring method, and distributed spring method. Reference [25] provides an extensive review of modeling techniques for offshore wind turbines on monopile foundations, considering foundation response under monotonic and cyclic loading. In [27], an overview is given of pile–soil interaction models under static and dynamic loading for various types of unfrozen soils.

The calculation approaches described are quite universal and can be applied to onshore wind turbines with various types of support structures. For example, in [28], coupled spring models are used for gravity-based foundations, while in [4], nonlinear distributed springs are employed as boundary conditions for simulating wind turbines on piles embedded in permafrost soils.

Grounds in Arctic regions are subject to seasonal changes and long-term degradation due to the permafrost thawing. At the same time, permafrost does not exist in all countries and is primarily found across large areas of Russia, the United States (Alaska), Canada, the Nordic countries, and the Chinese plateau [29]. As a result, only a limited number of studies incorporate the permafrost reaction into wind turbine models, which restricts the ability to assess dynamic loads and structural stability under realistic conditions. In [5], the results of field investigations of the dynamic response of a wind turbine on a pile foundation embedded in permafrost in Alaska are presented. It is noted that the ground stiffness varies due to seasonal and long-term temperature changes and permafrost degradation, which affects the overall stiffness and dynamic behavior of the structural system and can lead to resonance. In [4], numerical studies of the same wind turbine are presented, in which a foundation response model based on the average foundation temperature obtained from field measurements was used to describe the interaction between the foundation and the frozen ground.

However, studies on the supporting structures of Arctic wind turbines that account for foundation response derived from predictive thermophysical models are currently lacking.

Thus, the design of structures in Arctic regions requires the development of models for investigating thermophysical processes in permafrost foundations. Such processes are usually simulated using specialized tools for thermophysical modeling, such as Frost 3D, or universal finite element software packages like Midas GTS NX. These tools enable the simulation of soil temperature regimes, including heat and moisture transfer within the ground, while accounting for climatic factors, solar radiation, and the implementation of thermal stabilization systems. References [30, 31] provide examples of applying temperature regime modeling to assess temperature distribution within the ground.

The interaction between thermophysical and mechanical processes in the ground under structures with dynamic loads is partially discussed in [32–38]. Reference [32] notes that soils, like other materials, may experience heating under dynamic loading, which is likely one of the key mechanisms contributing to the degradation of permafrost properties under such conditions. At the same time, the pronounced creep behavior of frozen soils leads to a noticeable increase in their stiffness with higher loading rates. In [33], it is reported that frozen soils exhibit competing mechanisms: as the rate of dynamic loading increases, mechanical properties tend to decrease due to heating but simultaneously increase due to creep effects. Experimental studies focused specifically on temperature rise under dynamic loading are scarce in the literature; however, this effect is indirectly considered in studies of the dynamic elastic modulus of frozen soils. References [34, 35] provide an overview of experimental research on the behavior of frozen soils under dynamic loads. Empirical data show that the deformation modulus of frozen soils increases with decreasing temperature and increasing loading frequency, but decreases with increasing amplitude. Studies [36–38] present experimental data on the stiffness of pile foundations in frozen soils and propose mathematical models for calculating the parameters of nonlinear springs that simulate foundation response as a function of temperature.

However, studies that examine the conditions of fixation influence under potential permafrost degradation on the SSS and dynamic characteristics of Arctic wind turbines, including natural frequencies and resonance risk, are virtually absent.

The objective of this study is to develop an integrated methodology for analyzing the behavior of Arctic wind turbines under specific environmental and climatic conditions, based on the supporting structures SSS and dynamic response finite element modeling, considering wind and operational loads, nonlinear ground response and the thermophysical and mechanical properties of permafrost.

To achieve this objective, the following tasks were solved:

- a computational model of the wind turbine structural system was developed to simulate the SSS and natural vibrations of the supporting structures, considering nonlinear conditions of fixation;
- a model of nonlinear constraints for the wind turbine support structure was developed to calculate reactive forces in degrading permafrost under dynamic loading, incorporating soil properties and the thermal regime of the ground;
- a thermophysical model of the permafrost foundation was developed, considering the effects of air temperature, solar radiation, and thermal stabilization systems, to define nonlinear constraints parameters for the structural model of the wind turbine;
- an integrated methodology for modeling the supporting structures of Arctic wind turbines was formulated based on the developed models;
- the proposed methodology was tested through a case study of a 100 kW Arctic wind turbine with a 30 m tower and a 24 m rotor diameter, operating under the conditions of the Yamal-Nenets Autonomous Okrug.

## *2. Methods*

Modeling the supporting structural system of a wind turbine using finite element software for analyzing the SSS of structural components and the dynamic response of the structure under Arctic environmental conditions require consideration of wind-induced and operational loads, nonlinear ground response, thermal regime, and temperature-dependent soil properties.

Fig. 1 presents the scheme of loads and environmental impacts acting on the supporting structural system of the Arctic wind turbine.

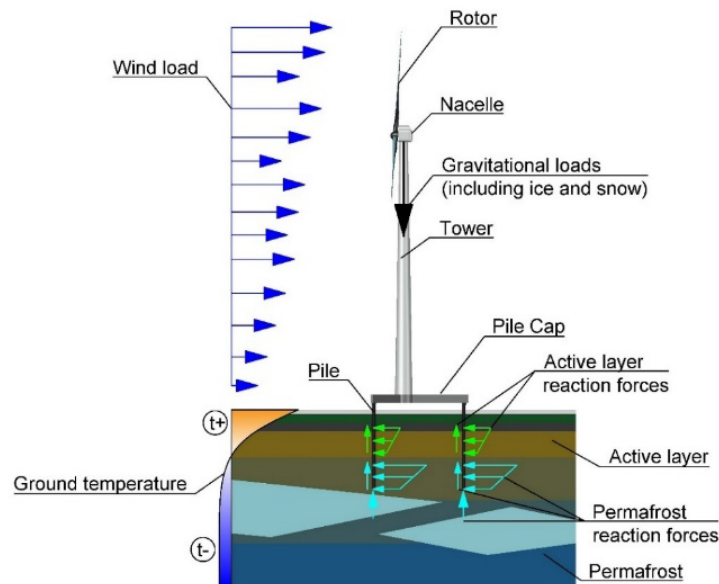


**Figure 1. Scheme of loads and environmental impacts on the supporting structural system of the Arctic wind turbine.**

A distinctive feature of the proposed methodology is its systemic approach, which includes thermophysical modeling of the "structure–ground" system, analysis of pile–soil interaction and detailed numerical modeling of the wind turbine supporting structures.

Fig. 2 presents the structure of the Arctic wind turbine supporting structures computational study.

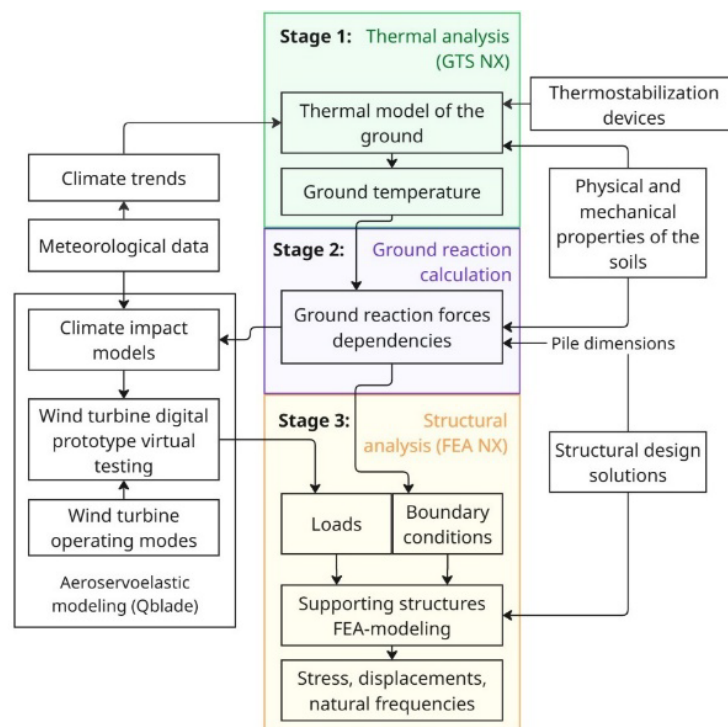


**Figure 2. Structure of the Arctic wind turbine supporting structures computational study.**

The computational methodology consists of three main stages:

**Stage 1: Thermal analysis with thermophysical modeling of the ground;**

**Stage 2: Calculation of the ground reactive force – displacement relationships considering temperature; Stage 3: Structural analysis, including the stress–strain state and determination of the natural frequencies and mode shapes of the wind turbine.**

At Stage 1, thermophysical processes in the permafrost ground are simulated to assess the temperature distribution in the soil, considering variations in air temperature, solar radiation, and the thermal stabilization systems. The finite element method (FEM), implemented in the GTS NX software package [39], is employed for this purpose. This approach enables consideration of the complex geometry of the

foundation and soil layers, the heterogeneity of thermophysical soil properties, and allows for the numerical solution of nonlinear equations, including the effects of phase transitions.

The following calculation scenarios are considered:

1. the site under natural conditions without accounting for the thermostabilization and climatic trends.
2. the site considering the structure with thermostabilization.
3. the site under natural conditions accounting for climatic trends.
4. the site considering both climatic trends and the structure with thermostabilization.

The thermophysical properties of structural materials and foundation soils are determined based on survey results or reference data.

Heat exchange with the atmospheric air throughout the year is modeled using a convective thermal boundary condition in accordance with the following formula:

$$q_a = \alpha \Delta T = \alpha (T_a - T_{sur}), \quad (1)$$

where  $q_a$  – heat flux from atmospheric air through the ground surface;  $\alpha$  – convective heat transfer coefficient, which depends on wind speed and the thermal conductivity of the snow cover;  $T_a$  – air temperature, which varies throughout the year;  $T_{sur}$  – ground surface temperature.

The heat flux received from solar radiation is described by the following formula:

$$q_s = G(1 - A), \quad (2)$$

where  $G$  – total solar radiation on a horizontal surface for the latitude in question, determined from reference data;  $A$  – surface albedo, taken as 0.9 when snow cover is present and 0.4 when it is absent.

To account for heat losses due to ground surface back radiation, evaporation, and to compensate for inaccuracies in the parameters of natural climatic conditions, a reduction coefficient  $k$  is proposed, determined through calibration of the thermophysical model. Thus, the total heat flux, considering solar radiation, can be represented by a temperature correction applied to the convective heat transfer boundary condition:

$$q = q_a + kq_s = \alpha \left( T_a - T_{sur} + k \frac{G(1-A)}{\alpha} \right) = \alpha (T_a - T_{sur} + kT_{corr}) = \alpha (T_{a.c.} - T_{sur}), \quad (3)$$

where  $T_{corr}$  – temperature correction that takes into account solar radiation;  $T_{a.c.}$  – corrected air temperature;  $k$  – calibration coefficient.

A numerical model of the ground in its natural state is created for parameter calibration, with parameters adjusted to ensure the condition of constant temperature in the permafrost soil at a depth of 15 m.

To simulate long-term degradation, corrections based on linear trends of climate change are introduced into the climatic parameters.

The result of the thermophysical modeling is the temperature distribution within the ground and its temporal variation, which enables the determination of the active layer thickness and the calculation of reactive forces exerted by the ground on the Arctic wind turbine supporting structural system.

At Stage 2, the calculation of foundation reactive forces resulting from the deformation of the supporting structures is performed. To model the foundation reactive forces considering the temperature distribution obtained at Stage 1, the distributed spring method is employed. The deformation of the springs is described using nonlinear force-displacement relationships in the corresponding directions. Three types of springs are used in the model:

- “p-y” springs – model the lateral resistance of the pile;
- “t-z” springs – model the axial resistance along the pile shaft;
- “Q-z” springs – model the axial resistance beneath the pile tip.

The parameters of the “p-y” springs are adopted according to Equation 4, which has been validated in [37] based on field tests of piles in frozen silty soils:

$$p = \frac{p_u}{2} \left( \frac{y}{y_m} \right)^{\frac{1}{3}}, \quad (4)$$

where  $p_u$  – ultimate lateral resistance of the pile;  $q_u$  – uniaxial compressive strength of the frozen soil;  $d$  – pile diameter;  $y$  – horizontal displacement of the pile;  $y_m = \varepsilon_{50} \cdot d$ ,  $\varepsilon_{50}$  – relative strain at 50 % of the frozen soil strength.

The ultimate lateral resistance  $p_u$  is determined using Equation 5 [36]:

$$p_u = 3cd + \sigma_v d + Jzc, \quad (5)$$

where  $\sigma_v$  – vertical stress at depth  $z$ ;  $c$  – soil cohesion;  $J$  – empirical coefficient, typically taken as 0.5;  $z$  – depth from the ground surface.

The “t-z” and “Q-z” springs parameters used to model the response of frozen soils are adopted according to the methodology described in [40], based on the values of the cohesion of frozen soil. Given the predominance of dynamic loads on the wind turbine supporting structures, the short-term value of the cohesion of frozen soil is used for extreme load cases and dynamic simulations.

The influence of temperature in the calculation of spring parameters is taken into account through the short-term cohesion of frozen soil,  $c_f$ , which is calculated using the formula provided in [41]:

$$c_f = c_t + \frac{\rho_w L_f}{T_f} (T_f - T)^{1-\alpha} \left( \frac{n - w_w}{n} \right)^\beta, \quad (6)$$

where  $c_t$  – cohesion of unfrozen soil;  $\rho_w$  – water density (1000 kg/m<sup>3</sup>);  $L_f$  – latent heat of phase transition (334 kJ/kg);  $T_f$  – soil freezing point temperature;  $T$  – temperature;  $n$  – soil porosity;  $w_w$  – unfrozen water content;  $\alpha$  and  $\beta$  – model parameters.

The damping coefficients for the springs are determined using the formula provided in [26]:

$$c_m = 2k_s \frac{\beta_m}{\omega}, \quad (7)$$

where  $\omega$  – wind turbine fundamental natural angular frequency;  $k_s$  – secant stiffness of the spring;  $\beta_m$  – hysteretic damping ratio, assumed to be 5 %.

The described mathematical model of ground response links thermal and mechanical processes through temperature-dependent material properties, enabling the assessment of foundation reactive forces under subzero temperatures for the design of structures on permafrost. This model can be applied in nonlinear static analysis of supporting structures as well as in aeroservoelastic simulations of wind turbines.

For modal analysis of the structural system and determination of the wind turbine natural frequencies, linearized springs are used, accounting for the expected deformation levels under dynamic loading during normal operation. To determine the expected deformation levels, the structural system of the wind power plant is analyzed with nonlinear springs under the maximum design load corresponding to normal power generation mode, after which the secant stiffnesses of the springs are evaluated.

The result of Stage 2 is the set of relationships between the foundation reactive forces and the deformations of the supporting structures.

At Stage 3, Arctic wind turbine supporting structural system finite element modeling is carried out using the FEA NX software package [42]. The calculation scheme of the wind turbine used for finite element analysis is shown in Fig. 3.

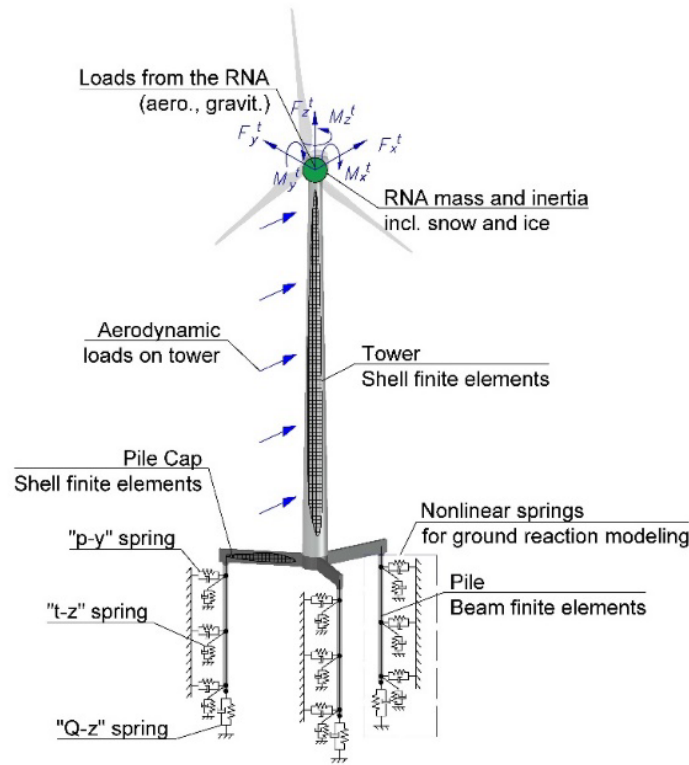


**Figure 3. Arctic wind turbine supporting structural system calculation scheme with nonlinear constraints.**

Since the subject of the study is the supporting structures, the RNA is modeled using an equivalent concentrated mass and inertia element. Loads from the RNA applied to the top point of the tower, taking into account natural climatic conditions and operational modes of the wind power plant, are determined based on aeroservoelastic simulations performed in the QBlade software package [13]. These loads are applied as a combination of forces and moments along six degrees of freedom (three forces  $F_x^t, F_y^t, F_z^t$  and 3 moments  $M_x^t, M_y^t, M_z^t$ ).

The stress and deformation analysis under extreme load combinations is conducted using a nonlinear static formulation. The governing equation of the problem can be expressed as:

$$[K]\{u\} = \{F_{ASEM}\}, \quad (8)$$

where  $[K]$  – stiffness matrix of the structural system;  $\{u\}$  – vector of absolute displacements of the structural system;  $\{F_{ASEM}\}$  – load vector determined based on the results of aeroservoelastic modeling.

Freezing and thawing of the soil change the mechanical properties of the ground, affecting the structural fixation conditions and its dynamic behavior. In the finite element model of the structural system, compliant boundary conditions are employed, with ground reaction modeled using single-node nonlinear springs whose parameters are defined based on the calculations from Stage 2. The problem, incorporating nonlinear spring parameters and geometric nonlinearity, is solved iteratively using a modified Newton–Raphson method.

For stress analysis under complex stress states, equivalent von Mises stresses are considered, generally defined by the following formula:

$$\sigma_{eq} = \sqrt{\frac{(\sigma_1 - \sigma_2)^2 + (\sigma_2 - \sigma_3)^2 + (\sigma_3 - \sigma_1)^2}{2}}. \quad (9)$$

Modal analysis is performed to determine the natural frequencies of vibration, with the governing equation expressed as:

$$([K] + \omega_i^2 [M])\{\varphi\}_i = \{0\}, \quad (10)$$

where  $\omega_i$  – natural frequency;  $[M]$  – mass matrix of the wind turbine;  $\{\varphi\}$  – eigenmode (mode shape) vector.

The supporting structural system above the ground surface is modeled using four-node shell finite elements. The interaction between the structure and the ground is modeled by representing piles with beam elements, which are connected to nonlinear springs simulating the soil reaction. In the model discretization, a mesh size of 0.01 m is used for the shell finite elements, while the pile beam elements are segmented with a step of 0.5 m.

Ice accretion on the blades and snow on the nacelle increase the mass of the wind turbine. To account for this in the modal frequency analysis of the supporting structures, two sets of equivalent mass and inertia parameters for the wind turbine are defined – one for normal conditions and one for conditions with snow and ice, according to the following formulas:

$$m_{RNA} = \sum m_i; \quad (11)$$

$$c_{RNAj} = \frac{\sum m_i c_{ji}}{\sum m_i}; \quad (12)$$

$$I_{RNAj} = \sum m_i r_i^2, \quad (13)$$

where  $m_{RNA}$  – mass of the RNA;  $m_i$  – mass of the  $i$ -th component of the RNA, including the mass of snow and ice;  $c_{RNAj}$  – coordinate of the wind turbine's center of mass along axis  $j$  relative to the top of the tower;  $c_{ji}$  – coordinate of the center of mass of the  $i$ -th component, including snow and ice mass, along axis  $j$ ;  $I_{RNAj}$  – moment of inertia of the RNA about axis  $j$ ;  $r_i$  – distance to the center of mass of the  $i$ -th component, including the mass of snow and ice.

Thus, two sets of mass-inertia characteristics of the RNA are considered, along with three foundation support conditions:

- under projected foundation degradation;
- in a thermally stabilized ground;
- under complete soil freezing (modeled as a rigid support at ground level).

Based on the results of the finite element analysis conducted at Stage 3, the following parameters are determined for the considered load cases:

1. maximum equivalent structural elements stresses and displacements, enabling the assessment of structural strength, identification of stress concentration zones, and evaluation of deviations from the design geometry.
2. natural frequencies and mode shapes of the Arctic wind turbine structure, allowing to assess the resonance risk at rotor and blade-passing frequencies.

### 3. Results and Discussion

The methodology was tested on an Arctic-designed wind turbine with a rated power 100 kW, a tower height of 30 m, nacelle dimensions of  $2 \times 1.3 \times 1.5$  m, and a rotor with a diameter of 24 m with an optimized blade shape developed by SPbPU for operation in Arctic conditions [43].

The supporting structural system of the wind turbine is made of S355 steel and includes a conical tubular steel tower and a three-point supported pile cap for loads transfer to the piles and ground. The top diameter of the tower is 1 m, the base diameter is 2 m, and the wall thickness is 10 mm. The pile cap consists of a tower mounting flange with a diameter of 2 m and a wall thickness of 30 mm, as well as 7-meter-long box-section beams with cross-section dimensions of 1000×320 mm, composed of 40 mm thick horizontal plates and 30 mm thick vertical plates. The pile cap is elevated and designed for construction on permafrost soils according to the principle of keeping frozen state of ground. The cap beams rest on bored-in-place circular steel piles with a cross section of 426×8 mm and a length of 11.5 m.



The scheme of the wind turbine under investigation is shown in Fig. 4, and the operating mode parameters are presented in Table 1.

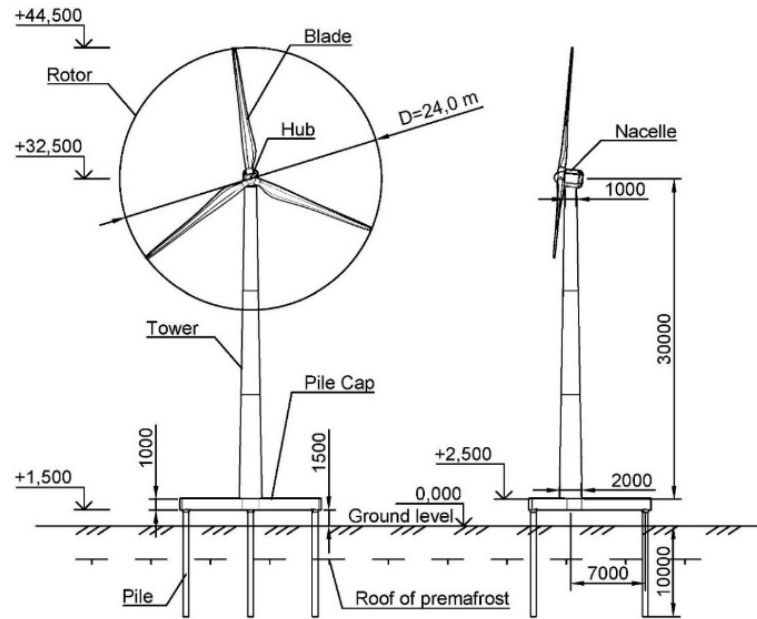


Figure 4. Scheme of the wind turbine under investigation.

Table 1. Wind turbine operation modes parameters.

Rated wind speed $V_r$	8 m/s
Rated tip speed ratio $\lambda_r$	8
Rotor rotational speed	variable from 0 to 75 rpm
Rated power of wind turbine $P_r$	100 kW
Operating wind speed range $V_{in} - V_{out}$	2–25 m/s
Orientation to the wind (yaw)	active, upwind
Power control	active, by rotating the blades (pitch control)
Control at extreme wind speeds	rotor stop, vane position of blades

The loads at the top of the tower were determined from aeroservoelastic modeling presented in [44] and are presented in Table 2.

Table 2. Loads from RNA on the tower top.

Load combination	$F_x^t$ , kN	$F_y^t$ , kN	$F_z^t$ , kN	$M_x^t$ , kNm	$M_y^t$ , kNm	$M_z^t$ , kNm	$F_{xy}^t$ , kN	$M_{xy}^t$ , kNm
Extreme mode	22.07	–12.25	–80.69	238.43	–10.72	–0.06	25.24	238.67
Normal operating mode	5.68	–0.88	–83.49	12.73	–9.25	3.96	5.75	15.74

To calculate the ground reactive forces, geological conditions obtained from engineering surveys for the construction of a wind-diesel power plant in the Yamalo-Nenets Autonomous Okrug (YaNAO) were used. The foundation consists of non-saline silty-sandy soils, classified into two layers, with their main characteristics summarized in Table 3. Thermal conductivity of the soils in frozen and unfrozen states, as well as the temperature-dependent unfrozen water content, were adopted in accordance with the regulatory guidelines of SP 25.13330.2020.

**Table 3. Permafrost soils characteristics.**

Layer number	1	2
Type of soil	Silty sand with silt inclusions	Silty sand with silt inclusions
Dry density $\rho_d$	1280 kg/m <sup>3</sup>	1550 kg/m <sup>3</sup>
Total moisture content $W_{tot}$	35 %	21 %
Freezing point temperature $T_{bf}$	-0 °C	-0 °C
Porosity coefficient $e$	0.99	0.72
Cohesion in unfrozen state $c_t$	5 kPa	10 kPa

According to the engineering survey data, the temperature of the permafrost (at the depth of zero annual temperature amplitude fluctuations, 15 m) was recorded as -0.5 °C, and the depth of the seasonally thawed layer was 2.2 m.

Air temperature and snow cover thickness were adopted based on data from the nearest meteorological station. Solar radiation was considered according to regulatory guidelines for the given latitude.

The annual variation of climatic parameters is presented in Fig. 5.

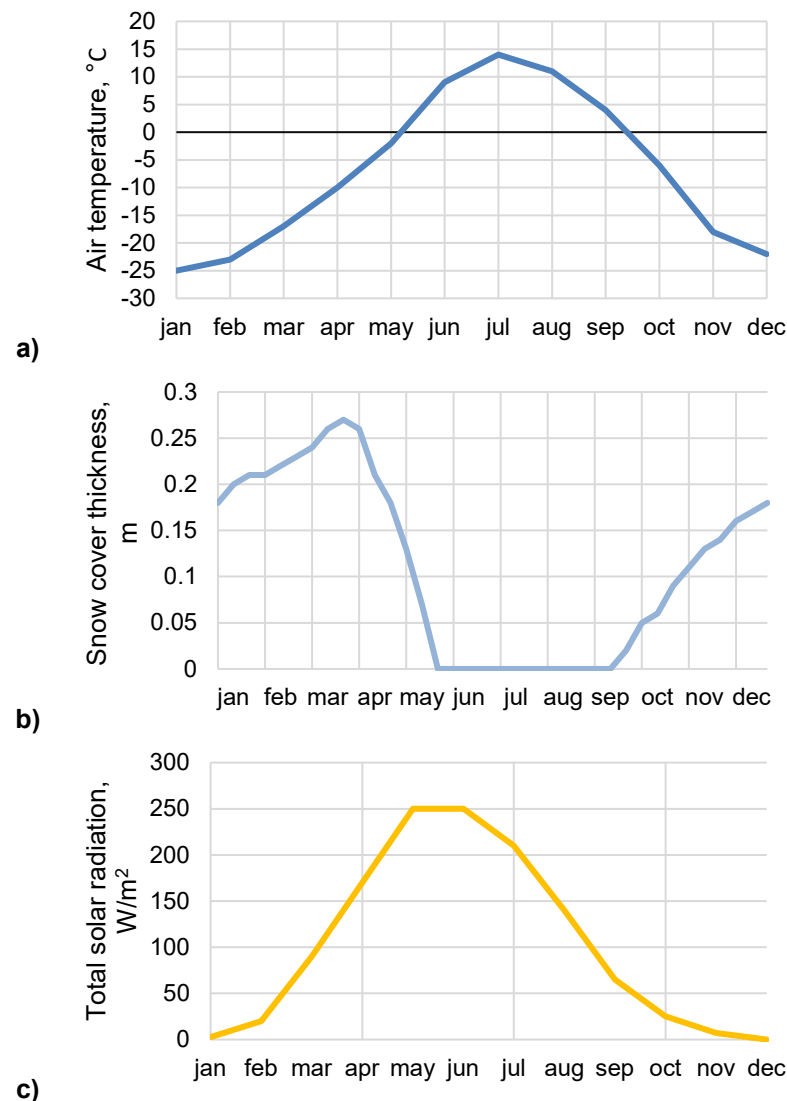


**Figure 5. Annual variation of climatic parameters:**  
a) air temperature, b) snow cover thickness, c) total solar radiation.

As a passive thermal stabilization system, a ventilated space above the foundation surface protected by a shielding screen on the pile cap is considered. The thermal stabilization effect is achieved by shading the foundation from solar radiation and maintaining an exposed (snow-free) soil surface during winter. In the thermophysical model, this is accounted for by an increased heat transfer coefficient in winter and the absence of solar radiation heat flux on the shaded area.

To model the global climate change, an increase in the average air temperature of  $0.71\text{ }^{\circ}\text{C}$  per 10 years and a 15 % increase in snow cover depth over 30 years were adopted, based on meteorological data [3].

The results of the thermophysical modeling at Stage 1 yielded the temperature distribution within the ground under various conditions.

Fig. 6 shows the temperature distributions along the pile after 20 years of wind turbine operation for various design scenarios.

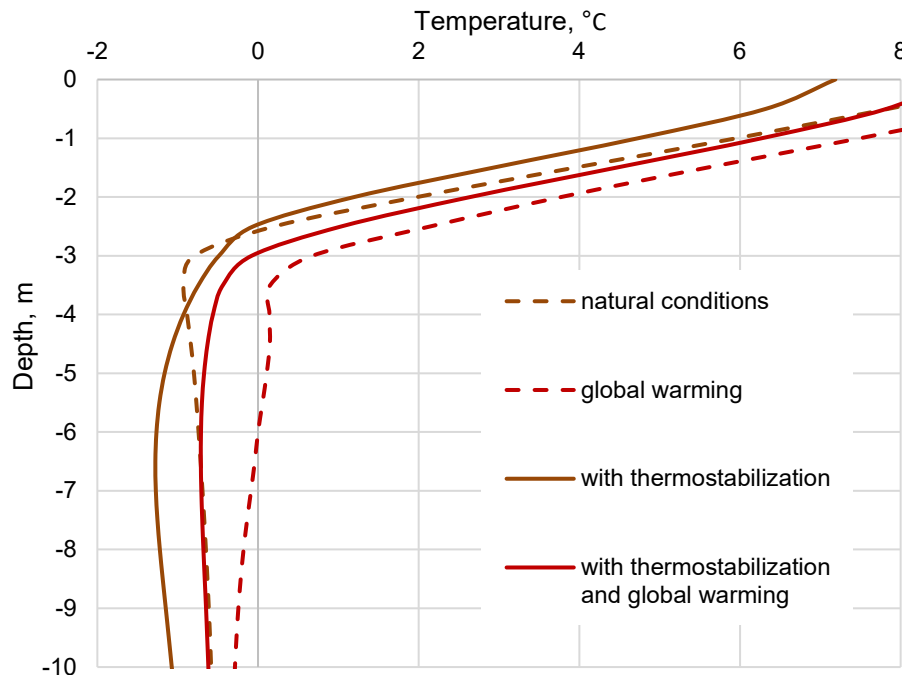


**Figure 6. Temperature distributions along the pile after 20 years of wind turbine operation.**

The modeling results show that the depth of seasonal thaw under natural conditions was 2.5 m, which closely corresponds to the engineering survey data. The presence of a pile cap with a shielding screen provided cooling of the foundation in August of the final year by  $0.3\text{--}2.4\text{ }^{\circ}\text{C}$  compared to the first year. This finding correlates with field studies of structures with ventilated spaces on permafrost [45], where a temperature reduction of  $0.6\text{--}2.5\text{ }^{\circ}\text{C}$  in the permafrost was observed for structures employing a similar thermal stabilization method.

When calculated with climatic trends considered, the thickness of active layer increased to 6 m by the end of the design service life of the wind turbine. The protective screen helped to offset the negative impact of warming and slowed permafrost degradation, ensuring stabilization of the annual average temperature with depth. At the same time, the thickness of the seasonally thawed layer at the pile location, considering the protective effect of the screen, was 3 m in the final year of operation.

The temperature distributions shown in Fig. 6 are used as input data at Step 2 for calculating the parameters of nonlinear springs modeling the reaction of the permafrost ground under loads from the structure. The primary calculation scenario assumes the temperature distribution considering both global warming and thermostabilization effects. Additional calculation scenarios include the temperature distribution with global warming but without thermostabilization, as well as rigid fixation of the piles at the ground surface to provide an upper bound estimate of the natural vibration frequencies in the case of increased foundation stiffness due to full freezing.

Fig. 7a presents a comparison of the calculated dependence of the soil cohesion on temperature with experimental data from [36]. Fig. 7b shows the temperature distribution along the pile length for the considered calculation scenarios.

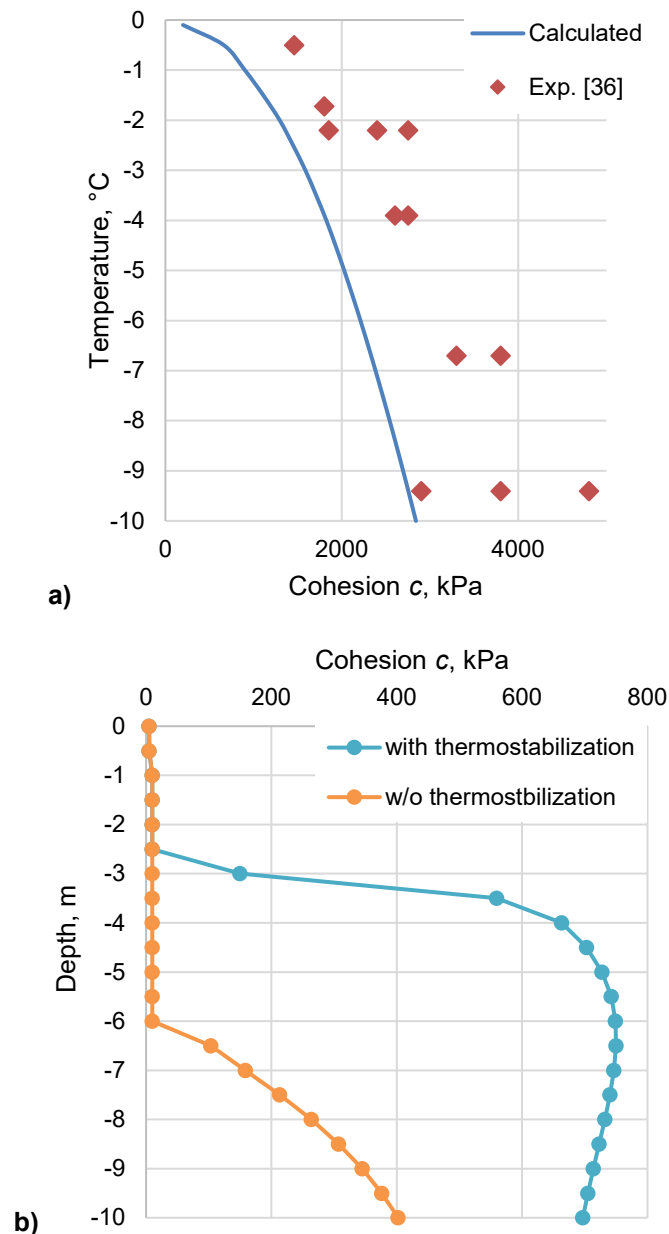


**Figure 7. Variation of soil cohesion: a) comparison of the calculated dependence of soil cohesion on temperature with experimental data, b) temperature distribution along the pile length.**

The analysis of the dependence of the frozen soil cohesion on temperature showed that the calculated estimates of cohesion do not exceed the values obtained experimentally. As the foundation temperature increases, the strength decreases exponentially, especially in the temperature range from  $-2^{\circ}\text{C}$  to  $0^{\circ}\text{C}$ , where intense melting of ice in the soil pores occurs. Within this interval, even a slight increase in temperature leads to a sharp reduction in strength.

Such behavior is reflected in the stiffness of the spring elements modeling the ground response. When the soil transitions from a frozen state at a temperature of  $-0.5^{\circ}\text{C}$  to an unfrozen state, the reaction forces of the soil at the same displacement decrease by a factor of 70.

Fig. 8 shows the “p-y” spring relationships describing the lateral resistance of the foundation at depths of 3, 6, and 9 m. With long-term degradation of the permafrost (scenario of  $+0.7^{\circ}\text{C}$  increase over 10 years), there is a systematic decrease in the stiffness of the ground, which should be taken into account when assessing the operational reliability of the wind turbine.

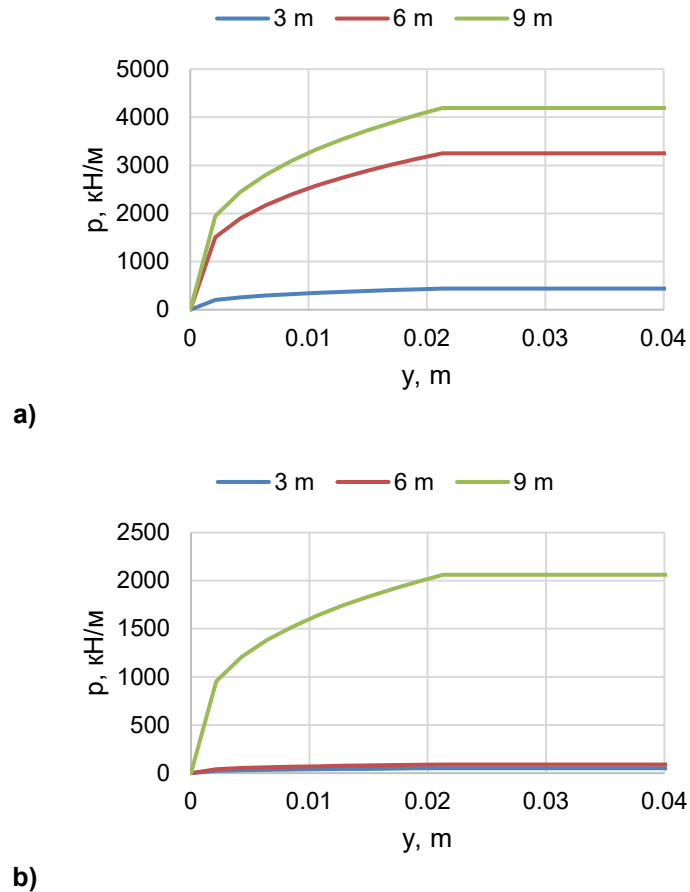


**Figure 8. Dependencies of foundation reaction  $p$  on horizontal displacement  $y$  along the pile: a) with thermostabilization, b) without thermostabilization.**

In the long term, cyclic wind and operational loads may induce cumulative effects such as progressive soil stiffening degradation and permanent settlements, which warrants further investigation as a direction for future research

At Stage 3, a finite element analysis of the wind turbine supporting structural system was performed for the extreme load combination (Table 3) based on three calculation schemes:

1. rigid fixation of the supporting structures at ground level (complete freezing of the ground);
2. nonlinear fixation of the supporting structures considering warming and thermostabilization;
3. nonlinear fixation of the supporting structures under warming without thermostabilization.

The results of the FEM analysis are the stresses and displacements of the supporting structures.

Fig. 9 shows the calculated absolute horizontal displacements of the tower, as well as the horizontal displacements relative to the tower base.

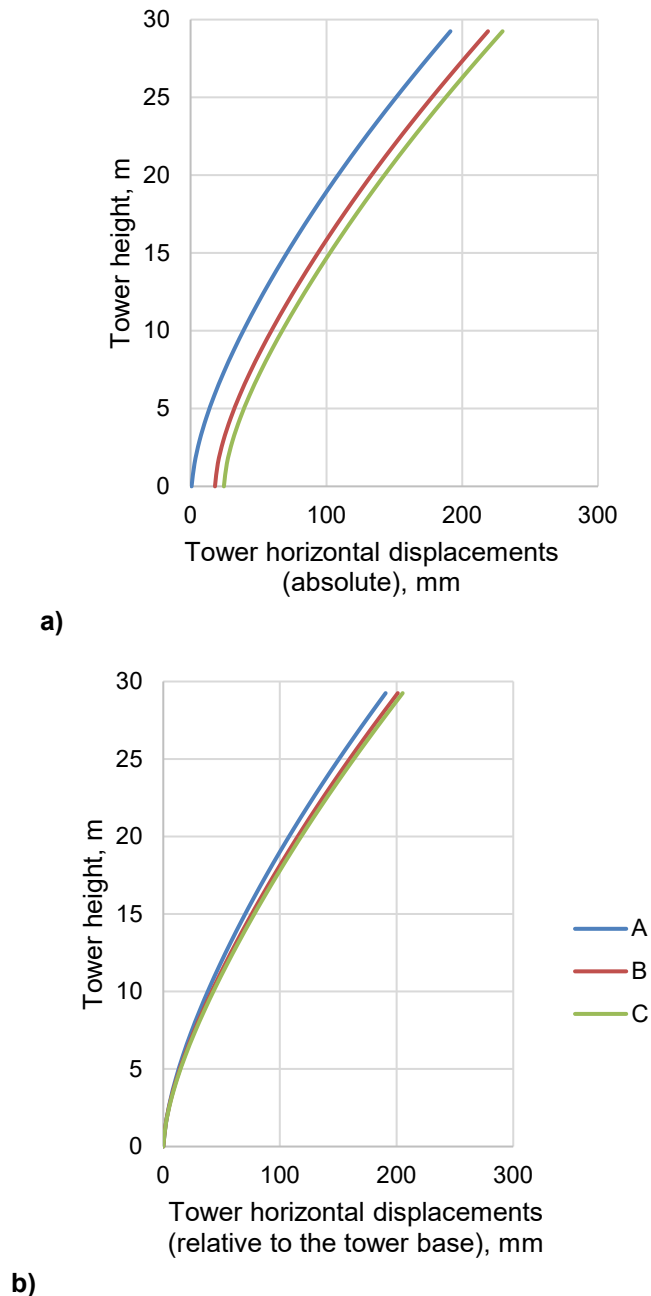


**Figure 9. Horizontal displacement of the tower in the calculation schemes A, B, and C:**  
**a) absolute, b) relative to the tower base.**

Fig. 10a shows that thawing of the ground leads to increased tower displacements. The main difference is associated with the displacement of the tower base due to reduced stiffness of the foundation: the displacements at the tower top increased by 14–20 % compared to rigid fixing, while the displacements of tower base increased by 24–33 times. The increase in horizontal tower displacements without thermostabilization ranged from 5 % to 37 % compared to the thermostabilized ground. The tower displacements relative to the tower base increased by 6–8 % compared to rigid fixing.

The study showed that permafrost degradation over the service life will not lead to a significant increase in internal forces and stresses within the tower material. However, a noticeable increase in absolute displacements under extreme loading indicates the potential for excessive amplification of the wind turbine vibration amplitudes.

To analyze the deformation of the pile cap, displacements at characteristic points were considered. Fig. 10 shows the layout of control points: point 0 lies along the tower axis and corresponds to the tower mounting flange located at the center of the pile cap, while points 1, 2, and 3 are located at the ends of the pile cap beams. The displacements at these points obtained from the analyses of schemes A, B, and C are presented in Table 4.

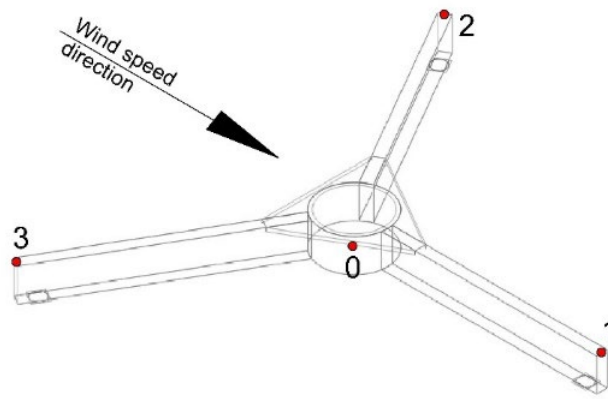


**Figure 10. Scheme of control points for monitoring pile cap displacements.**

**Table 4. Pile cap structural elements displacements.**

Structural element	Control point (Fig. 10)	Displacements in calculation scheme, mm		
		A	B	C
Tower mounting flange	0	0.17	17.5	24
Pile cap beam 1	1	0.79	17.06	23.6
Pile cap beam 2	2	1.74	14.44	20.05
Pile cap beam 3	3	2.5	12.7	17.89

From Table 4, it is evident that thawing of the ground leads to an increase in pile cap deformations. The displacements of the tower mounting flange increase by a factor of 10–14 when considering the compliance of the ground compared to the rigid fixation case. Overall, the pile cap displacements under the scenario without thermal stabilization (scheme C) are 40 % higher compared to the scenario with a thermally stabilized foundation (scheme B).

To assess the impact of ground thawing on the stresses in the supporting structures, the maximum equivalent stresses in structural elements were determined (Table 5).

**Table 5. Maximum equivalent stress in the wind turbine supporting structures.**

Structural element	Maximum stress $\sigma_{eq, max}$ in calculation scheme, MPa		
	A	B	C
Tower	167	167	167
Pile cap beam	144	174	180
Tower mounting flange	253	285	293
Piles	242	291	283

Based on Table 5, thawing of the foundation does not lead to a significant increase in stresses in the tower but it primarily affects the pile cap beams, the tower mounting flange and the piles. The maximum stresses at the supporting structure are 10–25 % higher when ground compliance is considered compared to the rigid fixation case. The greatest increase in stresses is observed in the pile cap beams. In all considered scenarios, the maximum stresses are localized at the tower mounting flange and at the points where the pile cap beams connected to the piles.

To analyze the dynamic response of the wind turbine, the inertial characteristics of the RNA were calculated both with and without the inclusion of additional masses of ice and snow (Table 6). These values were used to determine the natural frequencies of structural vibrations and assess the risk of resonance. The computed natural frequencies include bending modes along and across the wind direction (longitudinal and lateral), as well as the torsional mode, and are presented in Table 7.

**Table 6. RNA inertial characteristics.**

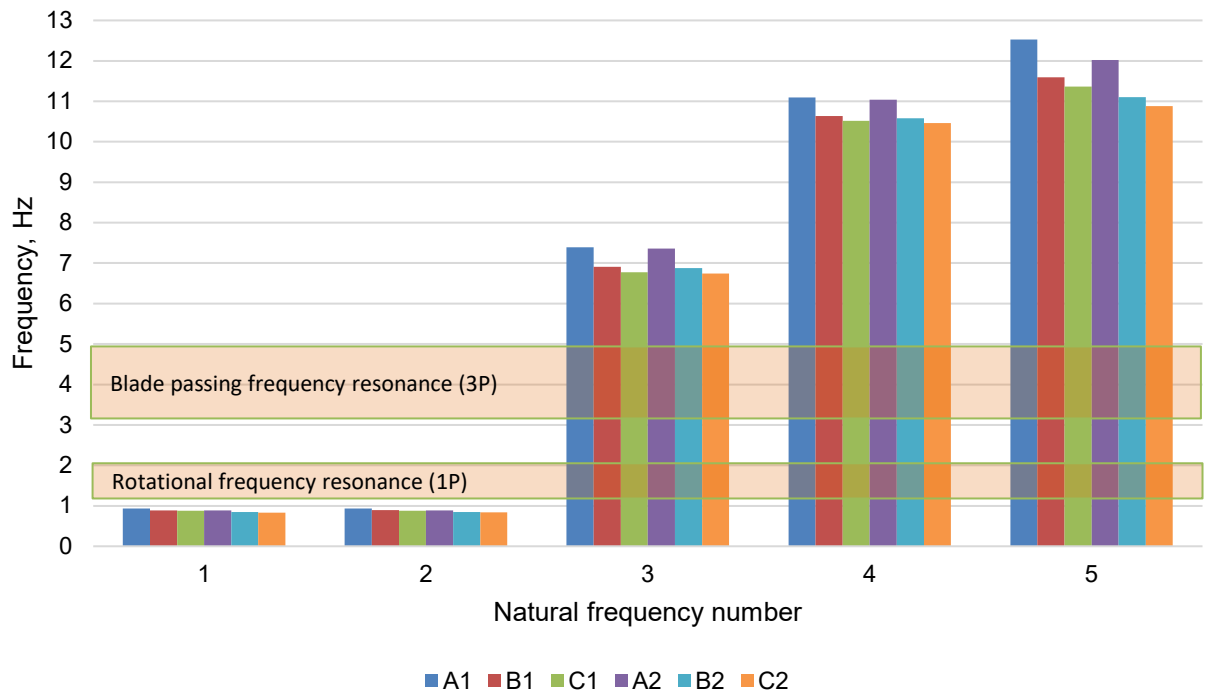
RNA inertial characteristic	1. Normal conditions	2. With ice and snow
RNA mass, kg	8500	9313
Coordinates $x, y, z$ of the RNA center of mass relative to tower top, m	(−0.327; 0.000; 0.750)	(−0.343; 0.000; 0.840)
Moments of inertia of the RNA inertia about axes $x, y, z$ , $\text{kg} \cdot \text{m}^2$	(37858; 20867; 23600)	(38574; 21092; 23792)

**Table 7. Wind turbine natural frequencies under various environmental conditions.**

No.	Mode of vibration	Natural frequency, Hz					
		Normal conditions			With ice and snow		
		A1	B1	C1	A2	B2	C2
1	Bending lateral	0.93	0.89	0.88	0.88	0.85	0.83
2	Bending longitudinal	0.93	0.89	0.88	0.89	0.85	0.84
3	Torsional	7.39	6.91	6.77	7.36	6.88	6.74
4	Bending lateral	11.09	10.64	10.52	11.04	10.58	10.46
5	Bending longitudinal	12.53	11.59	11.37	12.02	11.1	10.88

For the considered wind turbine, the presence of blade icing and snow on the nacelle reduces the natural frequencies of the structure by up to 5 %. Seasonal variation of the natural vibration frequencies due to thawing of the seasonal active layer reaches 4–7 % with thermostabilization and 6–10 % without it. This result is in good agreement with the findings of field and computational studies of an Arctic wind turbine with a similar configuration conducted in Alaska [4, 5], where a seasonal variation in the natural frequency of the tower-foundation system of up to 9 % was observed. Despite some differences in the parameters of the supporting structures of the considered wind turbine compared to those in [4, 5], this agreement indirectly validates the adequacy of the integrated methodology in assessing the variability of the structure's natural frequencies under permafrost degradation.

Fig. 11 shows the ranges of resonance frequencies and the natural vibration frequencies in accordance with Table 7.

**Figure 11. Ranges of resonance frequencies and the natural vibration frequencies.**

It can be seen from Fig. 12 that the natural vibration frequencies of the considered wind turbine do not fall within the ranges of dangerous resonance frequencies. The closest to the resonance frequencies are the natural frequencies in case A1 – when the ground is fully frozen and there is no snow load or icing.



It should be noted that snow loads and icing have the greatest effect on vibration modes 1, 2, and 5 (4–5 %), while having almost no effect on modes 3 and 4 (0.5 %). Ground thawing has the greatest impact on torsional vibrations (7 %). The highest amplitudes of torsional vibrations in cases B and C (with ground thawing) are observed at the pile cap beams ends, whereas in case A (rigid support), the highest amplitudes are localized at the top of the tower.

Based on the calculation results under various conditions, it has been established that accounting for additional ice and snow masses, as well as the permafrost degradation, enables a more accurate assessment of the stress-strain state and dynamic response of the wind turbine. These factors are particularly important for evaluating the natural frequencies of the structure and the stresses and deformations in the foundation structural elements, while having a secondary influence on the stresses in the tower. A more precise assessment of the SSS allows for a more accurate evaluation of the structural safety margins and the development of efficient structural solutions.

Accounting for the influence of Arctic climatic factors is crucial in aeroservoelastic modeling and in the development of resonance avoiding strategies. For example, when avoiding resonance by ensuring that the natural frequency of the wind turbine is lower than the rotor's rotational frequency ("soft-soft" strategy), and by tuning the control system to bypass resonant rotor speeds, a wider range of natural frequencies should be considered.

#### 4. Conclusion

1. An integrated methodology has been developed for Arctic wind turbine behavior analyzing under specific environmental condition, based on finite-element modeling of wind turbine supporting structures SSS and dynamic response considering wind and operational loads, nonlinear soil-structure interaction, thermal regime, and temperature-dependent soil properties.
2. Based on the case study of a 100 kW wind turbine:
  - it was established that without thermostabilization, seasonal thawing depth increases from 2.5 m to 6 m under climate trends, leading to a sharp reduction in soil strength within the thawed zone and a 70-fold decrease in ground reaction forces when transitioning from frozen to thawed conditions;
  - it was shown that permafrost degradation increases horizontal displacements of the tower by 14–20 %, and displacements of the tower mounting flange by 24–33 times; the degradation of the ground reduces the natural frequencies of wind turbine by up to 10 %;
  - it was found that blade icing and snow loads increase the mass and inertia of the wind turbine, reducing the supporting structures natural frequencies by up to 5 %;
  - it was demonstrated that the expected changes in natural frequencies during the wind turbine service life do not lead to resonance risks. The frequencies closest to potential resonance correspond to conditions of fully frozen foundation and absence of snow and ice loads;
  - it was revealed that the greatest increase in stresses in the structures due to ground thawing occurs in the foundation structures, particularly in the pile cap beams (up to 25 % compared to rigid foundation), while stresses in the tower remain practically unchanged.
3. It is demonstrated that accounting for additional masses and temperature-dependent ground stiffness is essential in aeroservoelastic modeling of wind turbines and in developing resonance avoidance strategies. The range of potential resonances should be expanded to account for variability in natural frequencies.
4. The derived relationships and results enable a more accurate assessment of the SSS and dynamic response of Arctic wind turbines, to develop rational structural solutions that ensure operational reliability in degrading permafrost conditions.

#### References

1. Minin, V.A., Tselishcheva, M.A. Wind resources of the Western sector of the Arctic zone of Russian Federation and possible areas of their use. *Arctic: ecology and economy*. 2023. 13(1). Pp. 72–84. DOI: 10.25283/2223-4594-2023-1-72-84
2. Akperov, M., Eliseev, A.V., Rinke, A., Mokhov, I.I., Semenov, V.A., Dembitskaya, M., Matthes, H., Adakudlu, M., Boberg, F., Christensen, J.H., Dethloff, K., Fettweis, X., Gutjahr, O., Heinemann, G., Koenigk, T., Sein, D., Laprise, R., Mottram, R., Nikiéma, O., Sobolowski, S., Winger, K., Zhang, W. Future projections of wind energy potentials in the arctic for the 21st century under the RCP8.5 scenario from regional climate models (Arctic-CORDEX). *Anthropocene*. 2023. 44. Article no. 100402. DOI: 10.1016/j.ancene.2023.100402
3. Kattsov, V.M., Akentyeva Ye.M., Anisimov, O.A., Bardin, M.Yu., etc. Tretiy otsenochnyy doklad ob izmeneniyakh klimata i ikh posledstviyakh na territorii Rossiyskoy Federatsii. Obshcheye rezyume [Third assessment report on climate change and its consequences in the Russian Federation. General Summary]. SPb.: Naukoyemkiye tekhnologii. 124 p.

4. Zheng, M., Yang, Z.(J.), Yang, S., Still, B. Modeling and mitigation of excessive dynamic responses of wind turbines founded in warm permafrost. *Engineering Structures*. 2017. 148. Pp. 36–46. DOI: 10.1016/j.engstruct.2017.06.037
5. Yang, Z.(J.), Still, B.A., Wait, I., Chen, G. Dynamic Responses of a Wind Turbine Founded in Warm Permafrost. *Journal of Cold Regions Engineering*. 2018. 32(4). Article no. 04018011. DOI: 10.1061/(ASCE)CR.1943-5495.0000169
6. Liew, M., Ji, X., Xiao, M., Farquharson, L., Nicolsky, D., Romanovsky, V., Bray, M., Zhang, X., McComb, C. Synthesis of physical processes of permafrost degradation and geophysical and geomechanical properties of permafrost. *Cold Regions Science and Technology*. 2022. 198. Article no. 103522. DOI: 10.1016/J.COLDREGIONS.2022.103522
7. Gantasala, S., Luneno, J.C., Aidanpää, J.O. Influence of Icing on the Modal Behavior of Wind Turbine Blades. *Energies*. 2016. 9(11). Article no. 862 DOI: 10.3390/en9110862
8. Li, F., Cui, H., Su, H., Iderchuluun, Ma, Z., Zhu, Y.X., Zhang, Y. Icing condition prediction of wind turbine blade by using artificial neural network based on modal frequency. *Cold Regions Science and Technology*. 2022. 194. Article no. 103467. DOI: 10.1016/J.COLDREGIONS.2021.103467
9. Sokolov, V.A., Strakhov, D.A., Sinyakov, L.N. Design of tower type structures to dynamic effects taking into account flexibility of the pile foundation and the base. *Magazine of Civil Engineering*. 2013. 4(39). Pp. 46–50.
10. Bondarev, D.E. Tuned mass damper for reduction seismic and wind loads. *Magazine of Civil Engineering*. 2024. 17(5). Article no. 12904. DOI: 10.34910/MCE.129.4
11. Wang, T., Zhong, W., Qian, Y., Zhu, C. Unsteady Blade Element Momentum Method. *Wind Turbine Aerodynamic Performance Calculation*. Springer. Singapore, 2023. 99–112. DOI: 10.1007/978-981-99-3509-3\_6
12. Anderson, C.G. *Wind Turbines: Theory and Practice*. 2<sup>nd</sup> ed. Cambridge University Press. Cambridge, 2025, DOI: 10.1017/9781009499040
13. Marten, D. QBlade: A Modern Tool for the Aeroelastic Simulation of Wind Turbines. PhD Thesis. Berlin, 2020. 187 p. DOI: 10.14279/depositon-10646
14. Jonkman, B., Platt, A., Mudafort, R., Branlard, E., Sprague, M., Ross, H. et al. OpenFAST/openfast: v3.5.3. Zenodo. 2024. DOI: 10.5281/zenodo.10962897
15. Brown, K., Bortolotti, P., Branlard, E., Chetan, M., Dana, S., de Velder, N., Doubrawa, P., Hamilton, N., Ivanov, H., Jonkman, J., Kelley, C., Zalkind, D. One-to-one aeroservoelastic validation of operational loads and performance of a 2.8 MW wind turbine model in OpenFAST. *Wind Energy Science*. 9 (8). Pp. 1791–1810, DOI: 10.5194/wes-9-1791-2024
16. Papi, F., Troise, G., Behrens de Luna, R., Saverin, J., Perez-Becker, S., Marten, D., Ducasse, M.-L., Bianchini, A. Quantifying the impact of modeling fidelity on different substructure concepts – Part 2: Code-to-code comparison in realistic environmental conditions, *Wind Energy Science*. 9 (4). Pp. 981–1004. DOI: 10.5194/wes-9-981-2024
17. Elistratov, V.V. Engineering Feasibility and Designing of Energy Systems Based on Renewable Energy Sources for Difficult Natural and Climatic Conditions. *Elektrichestvo [Electricity]*. 2023. 10. Pp. 4–21. DOI: 10.24160/0013-5380-2023-10-4-21
18. Elistratov, V.V., Panfilov, A.A., Petrov, S.G. The use of digital technologies in substantiating the energy and design parameters of the Arctic wind power plant. *Plumbing, Heating, Air Conditioning*. 2024. 6(270). Pp. 56–59.
19. Bolshev, A.S., Frolov, S.A., Kharseyev, A.Ye., Rozov, I.O. Raschet prochnosti osnovaniya arkticheskoy vetroenergeticheskoy ustanovki pri deystvii ekstremalnykh vneshnikh nagruzok [Arctic wind turbine foundation strength calculation under extreme external loads]. *Polyarnaya mekhanika: Sbornik dokladov VI Vserossiyskoy nauchno-prakticheskoy konferentsii s mezhdunarodnym uchastiyem [Polar mechanics. Proceedings of the VI All-Russian Scientific and Practical Conference with International Participation]*. Nizhny Novgorod: NGTU im. R.Ye. Alekseyeva, 2023. Pp. 87–97. DOI: 10.46960/polmech\_2023\_87
20. Wu, X., Zhang, X., Bhattarai, H.B. et al. Structural Behavior Analysis of UHPC Hybrid Tower for 3-MW Super Tall Wind Turbine Under Rated Wind Load. *International Journal of Concrete Structures and Materials*. 2022. 16. Article no. 52. DOI: 10.1186/s40069-022-00542-8
21. Al-Sanad, S., Parol, J., Wang, L., Kolios, A. Design optimisation of wind turbine towers with reliability-based calibration of partial safety factors. *Energy Reports*. 2023. 9. Pp. 2548–2556. DOI: 10.1016/j.egyr.2023.01.090
22. Partovi-Mehr, N., Branlard, E., Song, M., Moaveni, B., Hines, E.M., Robertson, A. Sensitivity Analysis of Modal Parameters of a Jacket Offshore Wind Turbine to Operational Conditions. *Journal of Marine Science and Engineering*. 2023. 11(8). Article no. 1524. DOI: 10.3390/jmse11081524
23. Kim, D.J., You, Y.S., Sun, M.Y. Variable Natural Frequency Damper for Minimizing Response of Offshore Wind Turbine: Effect on Dynamic Response According to Inner Water Level. *Journal of Marine Science and Engineering*. 2024. 12(3). Article no. 491. DOI: 10.3390/jmse12030491
24. Bergua, R., Robertson, A., Jonkman, J., Platt, A. Specification Document for OC6 Phase II: Verification of an Advanced Soil-Structure Interaction Model for Offshore Wind Turbines. Report number: NREL/TP-500-79938. National Renewable Energy Laboratory. Golden, CO, 2021. DOI: 10.2172/1811648
25. Jindal, S., Rahmanli, U., Aleem, M., Cui, L., Bhattacharya, S. Geotechnical challenges in monopile foundations and performance assessment of current design methodologies. *Ocean Engineering*. 2024. 310(1). Article no. 118469. DOI: 10.1016/J.OCEANENG.2024.118469
26. Xi, R., Xu, C., Du, X., El Naggar, M.H., Wang, P., Liu, L., Zhai, E. Framework for dynamic response analysis of monopile supported offshore wind turbine excited by combined wind-wave-earthquake loading. *Ocean Engineering*. 2022. 247. Article no. 110743. DOI: 10.1016/j.oceaneng.2022.110743
27. Wu, J., Pu, L., Zhai, C. A Review of Static and Dynamic *p-y* Curve Models for Pile Foundations. *Buildings*. 2024. 14(6). Article no. 1507. DOI: 10.3390/buildings14061507
28. Mawer, B.W., Kalumba, D. Stiffness considerations of local wind turbine gravity foundations. *Proceedings of the 1<sup>st</sup> Southern African Geotechnical Conference*. CRC Press. London, 2016. Pp. 31–36. DOI: 10.1201/b21335-8
29. Harris, S.A., Brouckov, A.V., Guodong, C. *Geokriologiya: kharakteristiki i ispolzovaniye vechnoy merzloty [Geocryology: Characteristics and Use of Permafrost]*. Vol 1. Moscow, Berlin: Direkt-Media, 2020. 437 p.
30. Zhaysambaev, E.A., Maltseva, T.V., Kraev, A.N. Calculation of the temperature condition of a thermostabilizable base with a single pile. *Construction and Geotechnics*. 2023. 14(4). Pp. 5–18. DOI: 10.15593/2224-9826/2023.4.01
31. Nikiforova, N.S., Konnov, A.V. Forecast of the Soil Deformations and Decrease of the Bearing Capacity of Pile Foundations Operating in the Cryolithozone. *International Journal for Computational Civil and Structural Engineering*. 2022. 18(1). Pp. 141–150. DOI: 10.22337/2587-9618-2022-18-1-141-150

32. Voznesenskiy, Ye.A. Dinamicheskaya neustoychivost gruntov [Dynamic instability of soils]. Moscow: URSS, LELAND, 2019. 263 p.
33. Zhu, Z., Kang, G., Ma, Y., Xie, Q., Zhang, D., Ning, J. Temperature damage and constitutive model of frozen soil under dynamic loading. *Mechanics of Materials*. 2016. 102. Pp. 108–116. DOI: 10.1016/j.mechmat.2016.08.009
34. Mirnyy, A.Yu., Idrisov, I.H., Mosina, A.S. Dinamicheskiye svoystva merzlykh gruntov. Chast' 1. Ispytaniya v rezonansnoy kolonke [Dynamic properties of frozen soils. Part 1. Resonant column tests]. *GeolInfo*. 2024. 6(1/2). Pp. 28–35 DOI: 10.58339/2949-0677-2024-6-1/2-28-35
35. Mirnyy, A.Yu., Idrisov, I.H., Mosina, A.S. Dinamicheskiye svoystva merzlykh gruntov. Chast' 2. Ispytaniya metodom trehnosnogo szhatiya [Dynamic properties of frozen soils. Part 2. Triaxial compression tests]. *GeolInfo*. 2024. 6(3). Pp. 24–32 DOI: 10.58339/2949-0677-2024-6-3-24-32
36. Crowther, G.S. Lateral Pile Analysis Frozen Soil Strength Criteria. *Journal of Cold Regions Engineering*. 2014. 29(2). Article no. 04014011. DOI: 10.1061/(asce)cr.1943-5495.0000078
37. Li, Q., Yang, Z.(J.). P–Y Approach for Laterally Loaded Piles in Frozen Silt. *Journal of Geotechnical and Geoenvironmental Engineering*. 2017. 143(5). Article no. 04017001. DOI: 10.1061/(asce)gt.1943-5606.0001556
38. Bekele, Y., Sinitsyn, A. O. Impact of Climate Change on Infrastructure in Longyearbyen. Case study of pile foundations on sloping terrains. SINTEF Academic Press. Oslo, 2020. 50 p. DOI: 10.13140/RG.2.2.33278.33601
39. MIDAS GTS NX. Integrated Solution for Ground Analysis. [Online]. URL: <https://www.midasuser.com/en/product/gts-nx/> (reference date: 16.12.2025).
40. ANSI/API. Recommended practice 2 GEO/ISO 19901-4. Geotechnical and Foundation Design Considerations. 1<sup>st</sup> ed. API. Washington, D.C., 2011. 26 p.
41. Tsegaye, A.B., Nordal, S., Simple Models for Frozen Soil. Modelling the Strength of Saturated Frozen Soil. Report number: NTNU report. Norwegian University of Science and Technology, 2015. 42 p. DOI: 10.13140/RG.2.2.25386.06088
42. MIDAS FEA NX. Elevating Design Excellence with Advanced Simulation. [Online]. URL: <https://www.midasuser.com/en/product/fea-nx/> (reference date: 16.12.2025).
43. Voinov, I.B., Elistratov, V.V., Keresten, I.A. et al. Profiling a Wind Wheel Blade Using Parametric Optimization and Computational Aerodynamics Methods. *Thermal Engineering*. 2024. 71. Pp. 513–522. DOI: 10.1134/S0040601524060053
44. Rigel, I.V., Elistratov, V.V. Support structure strength assessment based on aeroservoelastic modeling of an Arctic wind turbine, *Vestnik MGSU* [Proceedings of the Moscow State University of Civil Engineering]. 2025. 20(7). 1030–1050. DOI: 10.22227/1997-0935.2025.7.1030-1050
45. Hou, X., Chen, J., Sheng, Y., Rui, P.F., Liu, Y.Q., Zhang, S.H., Dong, T.C., Gao, J.W. Field observations of the thermal stability of permafrost under buildings with an underfloor open ventilation space and pile foundations in warm permafrost at high altitudes. *Advances in Climate Change Research*. 2023. 14(2). Pp. 267–275. DOI: 10.1016/j.accre.2023.03.004

#### **Information about the authors:**

**Ivan Rigel,**

ORCID: <https://orcid.org/0009-0003-0940-372X>

E-mail: [ivan.rigel@yandex.ru](mailto:ivan.rigel@yandex.ru)

**Viktor Elistratov, Doctor of Technical Sciences**

ORCID: <https://orcid.org/0000-0001-7051-6027>

E-mail: [elistratov@spbstu.ru](mailto:elistratov@spbstu.ru)

*Received 05.06.2025. Approved after reviewing 24.09.2025. Accepted 24.09.2025.*